UNCLASSIFIED

AD 268 280

Reproduced
by the

ARMED SERVICES TECHNICAL INFORMATION AGENCY
ARLINGTON HALL STATION
ARLINGTON 12, VIRGINIA

UNCLASSIFIED

ST. ANTHONY FALLS HYDRAULIC LABORATORY

UNIVERSITY OF MINNESOTA

Project Report No. 65

INTERFERENCE EFFECTS OF A STRUT
ON THE
LIFT AND DRAG OF A HYDROFOIL

Submitted by

LORENZ G. STRAUB

Director

Prepared by

J. F. Ripken

August 1961

Copy No. 128

ST. ANTHONY FALLS HYDRAULIC LABORATORY

UNIVERSITY OF MINNESOTA

Project Report No. 65

INTERFERENCE EFFECTS OF A STRUT
ON THE
LIFT AND DRAG OF A HYDROFOIL

Submitted by
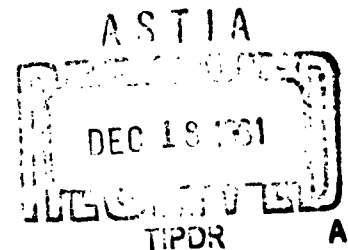
LORENZ G. STRAUB

Director

Prepared by

J. F. Ripken

ASTIA

DEC 19 1961

TIPDR   A

P R E F A C E

Although hydrofoil-supported, water-borne craft have been in ex-
istence for many years, it is only recently that an intensive effort has been
made to improve the understanding and design practices relating to such craft.

The current study of strut-interference effects is a small part of
this effort as sponsored by the Bureau of Ships, Department of the Navy. The
studies were carried out in the facilities of the St. Anthony Falls Hydraulic
Laboratory during the period October 1960 through August 1961 under Contract
Nonr-710(39).

Credit is due to J. M. Wetzel for advice throughout the program and
for critical review of the report, to A. N. Breivik for conduct of the test
program, to G. Subba Rao for data analysis, to L. J. Kirsch, N. M. Stuvetro,
and F. E. Thomas for fabrications and operations, and to Marveen Minish for
preparation of the manuscript under the general supervision of Loyal Johnson.

iii

A B S T R A C T

The evaluation of performance characteristics of hydrofoil systems employed to support water-borne craft commonly makes use of two-dimensional foil section analysis. Such evaluations are currently in need of more data for handling the contributions of the surfaces in the vicinity of the strut-foil junction where three-dimensional flow-interference effects occur.

In this study, towing tank tests were used to evaluate the influence of interference on the lift and drag of selected models of common junction conditions under a variety of submergence, attack, and yaw conditions. The evaluation was made from pressure distribution measurements.

C O N T E N T S

LIST OF ILLUSTRATIONS

Figure   Page

I̲N̲T̲E̲R̲F̲E̲R̲E̲N̲C̲E̲ E̲F̲F̲E̲C̲T̲S̲ O̲F̲ A̲ S̲T̲R̲U̲T̲
O̲N̲ T̲H̲E̲
L̲I̲F̲T̲ A̲N̲D̲ D̲R̲A̲G̲ O̲F̲ A̲ H̲Y̲D̲R̲O̲F̲O̲I̲L̲

I. INTRODUCTION

Hydrofoil systems for the support of water-borne craft frequently consist of submerged flat foils supported by vertical struts.

In the design of these foil configurations, extensive use has been made of the analogous theory and data previously developed for air-borne craft. The adoption of this related material has been very useful but has been limited to configurations operating with considerable submergence below the free water surface. This limitation applies because the proximity of the free water surface produces flow effects which depart from the infinite flow field normally employed by aircraft. This departure exists not only because of the general change in flow pattern which occurs above the foil but because of the secondary two-phase flow effects which may occur due to cavitation on the foil or air ventilation down the rear of the struts. The latter effects become increasingly serious as submergence decreases. To alleviate these effects, thinner foil and strut sections are employed and these in turn increase the structural problem and call for the use of an increased number of struts.

Since even a single strut-foil junction produces significant mutual interferences in the normal flow field around either member, the tendency to an increased number of junctions in the assembly will lead to substantial cumulative interference effects. Accurate analytical treatment of this complex three-dimensional condition is not yet available and design information must still be derived from experimental evaluations. A considerable amount of such empirical data has been accumulated for aircraft design [1]*, but in the newer field of hydrofoil-support structures the junction test data to date has been quite specific and not subject to broad application. Hoerner [2] summarised the available fragmentary data some years ago but there has been a continuous need for more interference tests directly involving the free-surface influence.

It is the purpose of this report to describe further tests which have been conducted at the St. Anthony Falls Hydraulic Laboratory. These were

---

*Numbers in brackets refer to the List of References on p. 16.

intended to assist in clarifying the strut interference effects relating to certain hydrofoil components, assemblies, and environmental conditions which were under design consideration. Because of the physical difficulties involved in making extensive small-force measurements in hydrodynamic systems, the range of coverage of these tests is fairly limited and not nearly as generalized as might be desired. It is hoped, however, that the data will serve to advance existing design information.

II. SELECTION OF HYDROFOIL TEST CONFIGURATIONS AND CONDITIONS

A. Foil and Strut Sections

Both the foil and strut section employed in these tests were arbitrarily selected from the NACA-1 series which is described in Refs. [3] and [4]. This series is designed to have the minimum pressure point unusually far back on both surfaces. This rearward position of minimum pressure provides a favorable pressure gradient, a laminar boundary layer, and an inhibiting influence on flow separation over an extensive area of the surfaces back from the leading edge. In addition, for design conditions, the magnitude of the lowest pressure value is greater with this type of foil than for conventional air-foil sections which normally produce a relatively low minimum pressure point near the leading edge. This higher value of the minimum pressure inherently affords a considerable protection against the inception of cavitation.

Because of the above-described properties, the NACA-1 series has been considered with interest for use in water-borne hydrofoil craft and was accordingly selected for use in this program. The foil selection was NACA 16-509, which is a section wherein the design minimum pressure point is back from the leading edge a distance which is 60 per cent of the chord.

The strut selection was NACA 16-012 and is a symmetrical section in which the design minimum pressure point is also back 60 per cent of the chord, but in which the maximum thickness is 12 per cent. This strut is somewhat thicker than needed for many applications but consideration has been given to designs which require interior space for housing of propulsive power shafting.

Sectional views of the 16-509 foil and the 16-012 strut are shown in Fig. 2 and coordinates for the surfaces of a 6-in. chord dimension are listed in Table I of the Appendix.

B. Foil and Strut Size

In the interest of providing design data involving a minimum of scale effect between the test and prototype configurations, a test assembly of maximum practical size was elected. For the available test facility and fabrication procedures, this leads to the arbitrary selection of a 6-in. dimension for both the foil chord and the strut chord.

C. Orientation

The geometry of the junction between the foil and the strut could have been arranged in a wide variety of relative placements. However, in the interest of simplicity in an initial program the placements were restricted to two fairly common forms. These consisted of a strut mounted at the extreme end of the foil and a strut mounted at the center of the foil.

Due to structural load limits of the type of fabrication employed, the foil span was also limited. This resulted in a final assembly in which the foil was supported and tested with the two end struts and one center strut in place at all times. The center distance between the end struts was 36 in. and between each end strut and the center strut the distance was approximately 18 inches.

In all tests, the axes of the struts were at 90 degrees with the foil chord line and with the axis of the foil. The leading edges of the struts were in a common plane with the leading edge of the foil.

D. Filleting

It has been established in aircraft studies that most of the detrimental drag effects associated with strut-foil junctions are due to the superimposed boundary layer influences at the junction corner. It has been further established that some of the detrimental effects may be materially reduced by filleting of the junction geometry. The aircraft filleted interference studies have indicated that optimum drag benefits are achieved by circular arc fillets having a radius of about 6 per cent of the chord with the filleting continuing beyond the trailing edges of the junction in a faired extension of appreciable length.

In an attempt to gain some insight into the influence of filleting on hydrofoil junction interference in a limited test program, tests were

conducted both with and without fillets. The fillets were in this case confined to one circular arc of 6 per cent radius with fillets not extending beyond the trailing edge. The fillets were maintained with a radius of 6 per cent between about the 10 per cent and the 90 per cent points along the foil chord. In the last 10 per cent of chord on each end the fillet radius was gradually reduced from a 6 per cent radius to a zero radius of arc, thus forming a gradually-faired transition in the junction.

For the end-strut tests, the fillets were placed only in the interior junction corner. For the center-mounted strut, fillets were placed on both sides of the strut.

E. Submergence Conditions

Earlier tests of flat hydrofoils have established that submergence of the foil to a depth of two or more chord dimensions will generally serve to eliminate the influence of the free surface on the hydrofoil performance. Below this depth, the hydrofoil will, in general, perform in accord with aircraft data relating to the infinite-fluid field. Above this depth, the foil is increasingly affected by the presence of the free surface. For very shallow submergence (a depth of 1/2 chord or less) and high speeds, the minimum pressure areas of the foil readily vent to the atmosphere and cause the performance characteristics to change drastically.

Because of these shallow depth difficulties, hydrofoil craft are frequently designed for an operating submergence of about one chord dimension.

In order to gain some insight into the influence of submergence on strut interference, the current test program employed two different submergence values. The selected depths were 100 and 200 per cent of the chord dimension.

F. Attack Angle Range

Interference effects for the tests were measured at foil attack angles of -4, 0, +2, +4, +6, +10, and, in a few instances, +15 degrees. The attack angles were measured between the chord line as shown in Fig. 2 and the horizontal water surface.

G. Yaw Angle Range

Interference effects for the tests were measured at foil angles of yaw of zero and 4 degrees in combination with most of the angles of attack

mentioned above. The yaw angle was in all cases applied such that the starboard end strut was trailed to the rear of the port strut during the test. The test data were then taken for conditions relating to the junction of the port strut with the foil. A comparable orientation was used for the center-strut tests and was considered to be the severest flow condition of the two alternates available for the unsymmetrical conditions of yaw.

H. Test Velocities and Model-Prototype Similitude

In order that model tests shall be meaningful to a prototype design, it is necessary that the dominant forces or flow patterns of the prototype shall be reasonably well-simulated in the model. In the case of a hydrofoil configuration operating near a free surface in a test channel, there are two criteria which are generally considered important to satisfy.

One criterion requires that gravitational or Froude number influences shall be similar. Since the prototype in this case normally involves high-speed motion in relatively deep water, the ratio of the body velocity to the velocity of the gravity wave will normally exceed unity. A rough approximation to this wave pattern will then occur if the model also produces a ratio or Froude number which exceeds unity. In the case of the current towing tests with a tank of 4.5-ft water depth, this will require that test body velocities shall exceed the wave velocity which is given by the expression

$$c = \sqrt{yg} = \sqrt{4.5g} = 12 \text{ fps}$$

A second criterion requires that viscous or Reynolds number influences shall be similar. In the case of flow over a foil, this is primarily a matter of maintaining the position of the laminar turbulent boundary layer transition such that any flow separations occur in essentially the same regions on model and prototype.

In the case of these selected NACA series 1 sections, which are of the so-called laminar-flow type, operation near the design attack angle of zero degrees should produce a laminar flow up to about the 60 per cent chord point. Because a favorable pressure gradient inherently exists ahead of the 60 per cent chord point, it may be expected that laminar flow will prevail to this point even for fairly high Reynolds numbers and modest surface roughnesses. However, deviations from the design attack angle or roughening of

the surface could cause wide variations in the location of the laminar-turbulent transition and consequent variations in performance. Some indication of the range of these variations was found in the hydrofoil data of Townsin [5] and a variety of related airfoil tests cited by Hoerner (Fig. 18, pp. 2-13, Ref. [1]). In some of these, transition occurred as early as $R_c = 8 \times 10^5$ and as late as $R_c = 10^7$. In light of this data, it appeared doubtful that artificial stimulation of the boundary layer would be meaningful to the current program unless conducted under a wider variety of conditions than the program permitted. In consequence, it was decided to abandon any attempt at artificial stimulation and to conduct all tests with smooth surfaces and related observations as to the position of the laminar-turbulent transition. This procedure was not considered a complete answer to the problem of simulating prototype flow but was intended to aid in defining the conditions of the model tests.

In light of the foregoing, it was decided that the tests should be conducted at the highest practical speed in excess of the critical Froude speed of 12 fps. However, the eventual fabrication technique employed for the hydrofoils resulted in a relatively weak structural assembly and need for low dynamic loading; as a result, it was finally decided to run all tests at a speed of 14 fps. This then resulted in a chord Reynolds number of about 7×10^5 for the tests.

III. TEST PROCEDURES AND FACILITIES

A. Type of Test

The physical evaluation of dynamic foil loads by towing procedures might normally employ either an appropriate dynamometer system or a pressure-distribution measuring system. In this instance, where the local forces sought are only a very small part of the total forces which can be readily measured, dynamometer methods present a serious problem. On the other hand, force measurements depending on surface pressure evaluations are incomplete in that they do not include shear force contributions. They also normally require considerable time and expense in data-taking and analysis. The pressure measurements do, however, provide detailed information on the mechanics of flow which are not apparent from bulk force measurements on a dynamometer. Such pressure information can be especially useful where it may be indicative

of values critical to the inception of such two-phase flow conditions as ventilation or cavitation. Since these criticals are common and vital to the normal performance of hydrofoils with shallow submergence, it was considered especially desirable to include them in these tests because the most critical pressures on the entire hydrofoil may be expected to occur in the strut junctions. Pressure-measuring facilities also have an advantage in that they are readily modified to permit boundary-layer-transition observations.

In light of this, it was decided to make the physical evaluation of forces by pressure-measuring procedures, despite the fact that the shear force contributions could not be measured by this procedure.

B. Foil Construction

Each foil and strut was composed of one large cast member, an end stack consisting of several thin sectional elements, and a junction piece. The junction piece and stacked sections were bolted to the end of the cast member. In each assembly one of the thin sectional slices contained a line of pressure-measuring holes in accord with the arrangement shown in Fig. 2. The assembly method permitted the line of pressure-measuring holes to be readily shifted axially along the member in the immediate vicinity of the junction. In addition to these tap-line positions, other lines were drilled directly into the main foil casting. The placement of these lines of pressure taps as used in the test program is shown in Fig. 3.

The large cast member contained brass tubing to serve as pressure transmission lines for the pressure taps together with other stiffening and tie rods. The member was cast in a carefully-screeded plaster mold using an alloy which melted at 160 F. Because of the low thermal levels and inherent nonshrink characteristics of the alloy, the casting was a very close copy of the mold.

The thin sectional elements were made of brass using a single hand-made master unit which was used as a template for profile machining of additional units. The stacked units and casting were then hand-finished to a smooth faired surface.

Pressure transmission passages through the stack were sealed with "O" rings.

8

C. The Towing Tank

The towing tank consisted of a concrete channel of 9-ft width, 6-ft depth, and about 210-ft length. The normal water depth in the channel was 4.5 ft and the temperature of the fresh water was 72 degrees throughout the tests. The tank walls were capped with rails to support the towing carriage.

D. The Towing Carriage

The towing carriage was propelled by trolley-fed electric driving motors. The acceleration conditions for the carriage at the selected 14 fps test speed provided 112 ft, or 8 sec, of stable test run.

The hydrofoil assembly was mounted below the carriage on a special support system which permitted ready adjustment of the submergence, attack angle, and yaw angle.

The general arrangement of the towing carriage and mounted foil assembly are shown in Fig. 1.

E. Pressure-Measuring Procedures

The pressure-measuring holes shown in Fig. 2 were connected to an external mercury manometer bank by pressure-transmission tubes contained within the foil and strut assemblies. Preliminary tests indicated that the pressure-stabilization time for the transmission system and manometer bank was approximately 20 sec for the test velocity of 14 fps. Since the towing tank length limited test conditions to an 8-sec run, the manometer system was provided with shut-off valves which were ganged and automatically tripped to be open only during the period when test velocities were in effect. Under these conditions, three successive towing tank runs were required for stabilization of the manometers representing any given test condition.

Because of the cost which would be associated with a manometer system involving the reading and plotting of thousands of individual pressure values, a simplified manometer system was evolved for the readout. This consisted of grouping the manometer tubes in their normal placement along a simulated chord line in a manometer board constructed to be transparent. The mercury columns representing pressure values on this board then appeared as a bar graph relative to the chord line. Exposure of a standard Verifax photocopy sheet behind the board directly provided a work sheet on which the full pressure distribution curve could be manually faired-in across the bar graph. These curves were then used for analysis of forces.

The turbulence and wave action produced in the tank by one towing run proved to have no effect on the pressure values of rapidly-repeated subsequent runs except for the maximum attack angle and yaw angle conditions. For these cases, a slight wave-quieting time was provided.

It may be noted that no cavitation or venting of the foil was observed for any of the environmental conditions imposed in these tests. Ventilation did occur down the rear of struts but appeared to be limited to depths of not more than 1/2 chord, and then only when tests involved both maximum yaw and maximum attack angle.

F. Visual Transition Observations

As pointed out in the discussion under section II-H, relative to boundary layer transition conditions, it is desirable to establish the position of the transition for effective extrapolation of the model data to the prototype.

Visual observations relative to the transition were made by secreting a dye material from a forward pressure hole in the foil and noting the chord point at which laminar breakdown occurred in the dye filament. These observations were confined to the line indicated as D in Fig. 3 and were run only for conditions of 200 per cent submergence, zero yaw, and the smaller design angles of attack.

IV. TEST DATA AND ANALYSIS

The various test conditions and the testing procedures used to obtain the pressure distribution curves were described in section III. Since the most meaningful results from these curves are the values of the lift and drag coefficients, the data-handling largely related to the determination of these coefficients. This was accomplished by area planimetering of the faired curves of the photo work sheets, thus providing direct evaluation of the normal lift coefficient, C_n. A graphical rearrangement of the bar graph indications on the photo work sheet also permitted plotting of the drag pressure diagram followed by area planimetering and similar evaluation of the chordwise drag coefficient, C_c.

From these two measures of the force components the conventional coefficients were computed thus:

$$C_D = C_n \sin \alpha + C_c \cos \alpha$$

$$C_L = C_n \cos \alpha - C_c \sin \alpha$$

It should be noted that space limitations restricted the number of pressure taps that could be placed near the leading and trailing edges of the test members. As a result, there was some obscurity as to the shape of the pressure diagrams in these areas. This limitation did not seriously affect a meaningful determination of the value of C_n but did make it difficult to achieve high accuracy in evaluating C_c. As a result, the values for C_L are considerably more accurate than those for C_D. This scarcity of taps also led to peak negative pressure measurements which were probably somewhat less than the true peaks for some tests.

In the original test planning it was arbitrarily assumed that a pressure profile taken at line D in Fig. 3 (positioned one chord dimension from the centerline of the junction) would probably be beyond the range of major interference effects and might be assumed as a reference profile. It could not be assumed that a two-dimensional flow prevailed in this plane but it seemed probable that it was as representative of near two-dimensional conditions as could be obtained from the configuration.

As a check on the above assumptions of flow character at line D, limited pressure values were also taken at lines L, M, and N. These values were combined with complete pressure measurements from lines A, B, and D to yield the summary graph plotted in Fig. 4. Unfortunately, the three-dimensional flow conditions and steep pressure gradients in the vicinity of the limited taps at L, M, and N do not completely validate line D as a reference section. A similar graph for the conditions prevailing near the center strut is plotted in Fig. 5.

The data of Fig. 4 is the basis for the following assumptions:

(a) The junction interferes or produces major force influences on the adjacent members for a member length equivalent to about 2/3 chord dimension.

(b) The mean coefficient of lift or drag applying to the inter- fered surfaces may be estimated by assuming that the values

for a given pressure line are applicable for an area up
to the center point of the space between adjacent pressure
lines.

(c)   The determination of interference length in accord with
(a) above and of mean force coefficient in accord with (b)
above is assumed to apply to center strut interference as
well as end strut interference.

Force coefficient values from the foregoing procedure for evaluating
interference influences on the foil have been graphically summarized in Figs.
6 through 9 for design use. These figures are arranged to permit selection
of appropriate force coefficients for the range of conditions and configura-
tions covered by these tests. For reasons of economy, the data of Figs. 6
through 9 are complete only for the reference condition of yaw equal to zero
degrees and submergence equal to 200 per cent. For most other conditions
only the design angle range from zero to 4 degrees has been calculated.

Although the foregoing determination of force coefficients is proba-
bly the most useful product of the test program, there is also considerable
information to be gained by an examination of the actual pressure distribution
curves. Certain of this type of data have already been graphically summarized
in Figs. 4 and 5. Additional data of this character are shown in Figs. 10,
11, and 12 for pressures at the reference lines D, B, and C. The latter
two curves represent foil conditions for measurements made as near as possible
to a filleted strut. A survey of the data shows that for the end strut the
minimum pressure is not as low as for the center strut and the end strut with-
out fillet has a slightly lower pressure than the end strut with fillet.

The visual observations of the position of boundary layer transition
are summarized in the graphical offering of Fig. 13. The indicated conditions
correspond to the pressure curves which were plotted in Fig. 10.

V.   COMPARATIVE VALUES FOR THE TEST DATA

As a check on the validity of the adopted method of evaluating the
interference effects and as a means of extending the ultimate design useful-
ness of these evaluations, comparisons with other findings were considered
desirable. Very little comparative material was available for these rather
uncommon NACA sections, but two approaches were considered of possible value.

One approach was the use of the original work by Stack [3], which included wind tunnel evaluation of the lift and drag coefficients for total lift of the 16-509 foil in the infinite flow field. These data are shown in Fig. 14 in comparison with the values taken from the test data for piezometer line D as shown in Fig. 3. Also included is a curve for wind tunnel data corrected to an arbitrary aspect ratio of 3. It is to be noted that the hydrofoil test data do not include the viscous shear forces which are inherent to the total force measurements of Stack.

A second useful comparison can be made between the pressure distributions measured in the test program and the theoretical approximation to this distribution. The theoretical distributions in this case were computed in accord with the procedure described in Ref. [4], pp. 75-79. For purposes of the calculations, an aspect ratio of 3 was arbitrarily selected. Comparative plottings of these pressure distributions are shown in Fig. 15. These plottings again include only the test data from pressure tap line D as shown in Fig. 3.

VI. DISCUSSION

A comparative study of the pressure profiles of Figs. 10 and 15 discloses the following interesting points with regard to the application of the laminar-flow type of foil section to a hydrofoil assembly:

(1) Despite the fact that a truly two-dimensional flow does not exist for the measurements made at tap line D in Fig. 15, the general shape of the pressure profile is in fairly good agreement with the theoretical distribution for the design angle of zero degrees.

(2) For an attack angle greater than 2 degrees, Fig. 10 shows the point of minimum pressure shifting from the 60 per cent chord position consistent with the designed laminar-flow section to a point near the leading edge. The latter is more in accord with the position on a conventional section. Fig. 13 indicates that some transition instability may exist for the test data of Fig. 10 for attack angles between 2 and 6 degrees.

(3) The shift in the position of the minimum pressure point as discussed in item (2) above is accompanied by a substantial reduction in minimum pressure values. The lowest of these values may serve as a rough measure of the critical cavitation limits for operation of the foil since the magnitude of the critical cavitation sigma is the same as the minimum pressure coefficient. It should be noted that because of the limited pressure taps and steep pressure gradients existing near the leading edge, the observed minimum pressures are not necessarily the least that exist.

(4) Fig. 10 indicates that stall or major separation of flow apparently does not occur below the 15-degree maximum attack angle tested, although the rise in minimum pressure between the 10- and 15-degree attack angles suggests that a local flow separation and subsequent reattachment may have taken place near the leading edge.

The polar plot of Fig. 14 indicates that the laminar flow foil in the three-dimensional configuration achieves a high lift-drag ratio over a more limited attack angle range than is the case in two dimensions. It should be noted, however, that the three-dimensional data do not include the shear force effects which are included in the total drag of the two-dimensional data.

A study of the pressure profiles of Figs. 4, 5, 10, 11, and 12 for design angles of attack indicates that the point of minimum pressure on the foil surface tends to move forward and to diminish in value as the junction is approached. This is true for both the junctions without fillet, as shown in Figs. 4 and 5, and junctions with fillet, as shown in Figs. 11 and 12.

It should be emphasized that the data relating to minimum pressure values should be used with caution. These data were obtained from a limited set of pressure taps which in all probability did not include the point of lowest pressure on the junctions. Moreover, the minimum value will vary considerably with the geometry of the particular junction. In view of this, the values are offered as a rough guide to the magnitude of the sigma value for the inception of cavitation but are not considered suitable for final design purposes.

The mean force coefficient values for the interfered surfaces of the foil are summarized in Figs. 6 through 9 to show the comparative influence of yaw angle, submergence, and filleting. A study of this data establishes that these three geometric factors do have a substantial influence on the force values but the complexity of the resulting flows fails to produce regular and systematic force changes when more than one factor is varied. However, for the low values of attack angle used in normal design practice and for practically all conditions tested, the curves do show a definite and substantial increase in lift and drag for the interfered surfaces. The magnitude of this increase may be approximated for the specific conditions by interpretation of the curves. Since the curves consist of pressure force data without shear force, two reference curves have been added to each graph. These give the comparative values for pressure forces on measuring line D and the comparable values for total forces for the infinite span and infinite flow field as taken from Ref. [3].

It should again be noted that the force values relating to yaw conditions apply to only one direction of yaw angle. Significantly, different values might occur for the opposite direction of yaw.

VII. CONCLUSIONS

An arbitrary selection of hydrofoil systems has been subjected to a limited range of noncavitating, nonventilating tests and analysis with the objective of obtaining force data for design use. The resulting force data findings have been summarized in Figs. 6 through 9. While these data are by no means comprehensive, they do supply information on a substantial range of conditions pertinent to design practice.

The following conclusions relate to these force findings:

(1) Due to limitations of the pressure-force-measuring procedures employed in the tests, the figures do not directly yield a handbook type of design data. However, use of the data in combination with related wind tunnel total force measurements, which are included, does permit a rational tie with other design procedures.

(2) The laminar-flow type of section elected for these tests was observed (Fig. 13) to provide laminar flow over the

forward area for only a relatively small attack angle
range. Increasing values of the chord Reynolds number
diminished this attack angle range. For prototype design
purposes involving high Reynolds numbers, these data are
then most useful for attack angles near zero degrees or
in excess of 6 degrees. Since transition variables may
occur for angles between zero and 6 degrees, data in this
region should be used conservatively.

(3) Stall or major separation of flow failed to occur on these
configurations for the attack angles of 15 degrees and less
which were tested.

(4) For design angles of attack, the interference of a strut
on a foil is such that a definite and substantial increase
in lift and drag occurs over the interfered portion of the
foil. This increase may diminish with increasing angle of
attack or yaw.

(5) The strut interferes or produces major force influences
on the foil for a foil length extending outward from the
junction for a dimension equivalent to about 2/3 chord
lengths.

(6) The use of fillets in the junctions produced only rela-
tively small interference force changes. The changes were
both positive and negative in value depending on the attack
angle and submergence conditions.

(7) For design angles of attack, the interference lift and drag
forces tended to diminish with decreasing submergence.

The point of minimum pressure on the foil tended to move forward
and to diminish in value as the junction was approached. This was true for
both end and center struts and with and without fillets (Figs. 4, 5, 11, 12).
The inception of cavitation on these foil assemblies may, therefore, be expected
in the forward part of the strut-foil junction and the related cavitation
sigma value may be approximated by the minimum pressure coefficients (Figs. 4,
5, 11, 12). The absence or presence of filleting produced relatively little
change in the minimum pressure value.

L I S T   O F   R E F E R E N C E S

[1] Hoerner, S. F. Fluid-Dynamic Drag. Published by the author. Section VII. 1958.

[2] Hoerner, S. F. The Influence of End Plates, Struts and Nacelles Upon the Characteristics of Hydrofoils. Technical Report No. 14, Gibbs and Cox, Incorporated. August 1953.

[3] Stack, J. Tests of Airfoils Designed to Delay the Compressibility Burble. National Advisory Committee for Aeronautics, Report No. 763. 1943.

[4] Abbot, I. H. and Von Doenhoff, A. E. Theory of Wing Sections. Dover Publications, New York. 1959.

[5] Townsin, R. L. "Experiments with a Low Drag Hydrofoil," Proceedings of the Institute of Naval Architects. 1955.

F I G U R E S
(1 through 15)
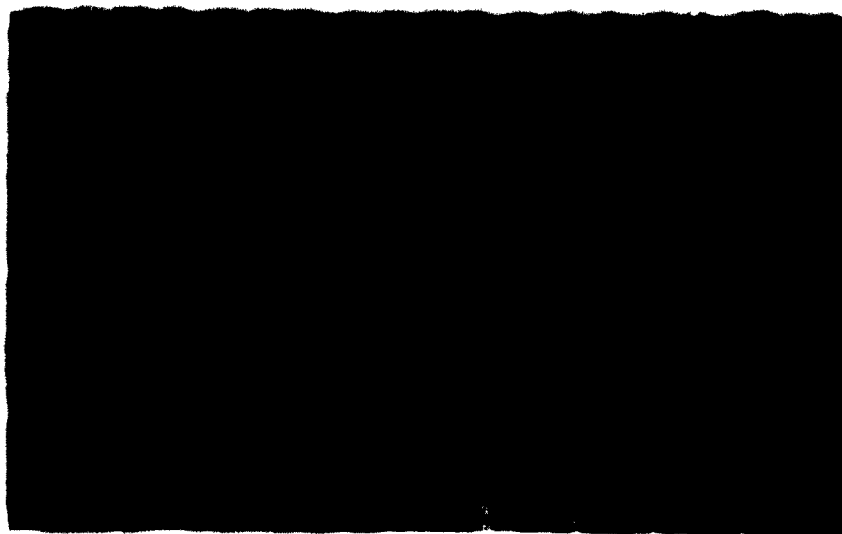
(a) THE TOWING FACILITY
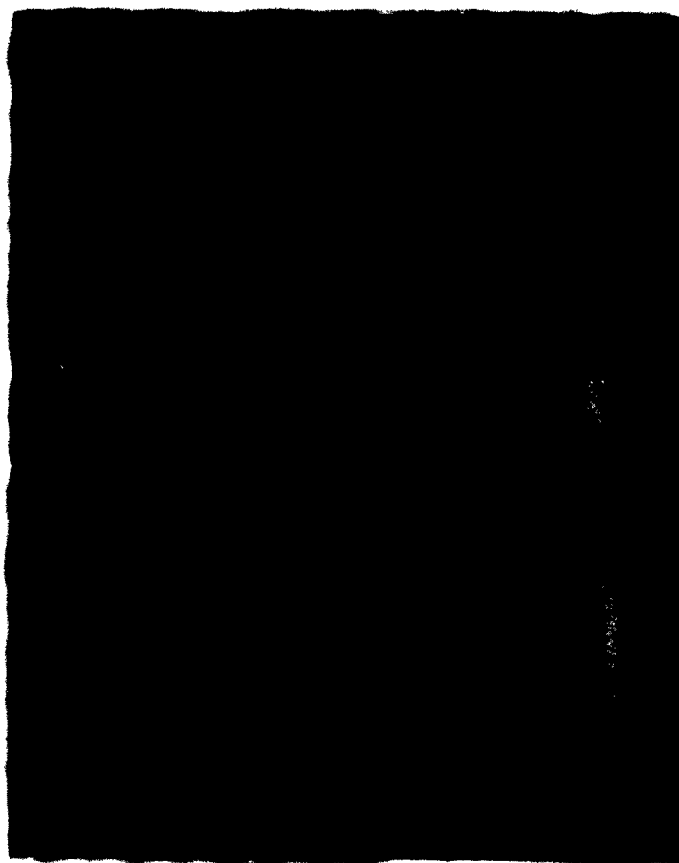
(b) THE HYDROFOIL ASSEMBLY

Fig. 1 — The Hydrofoil Testing Assembly
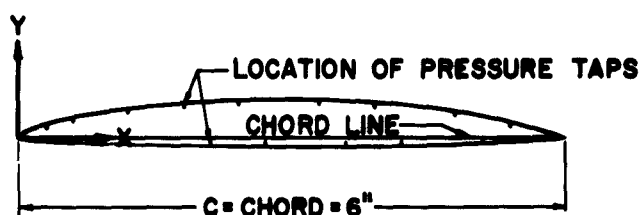
FOIL SECTION — NACA 16-509
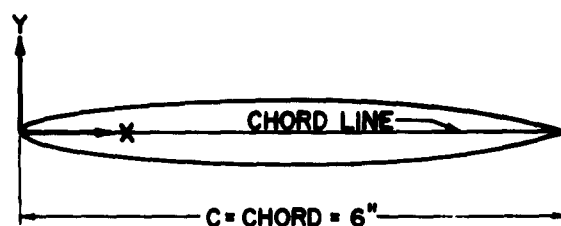
STRUT SECTION—NACA 16-012

NOTE: NUMERICAL VALUES FOR THE SURFACE COORDINATES
AND TAP LOCATIONS ARE GIVEN IN TABLE I.

Fig. 2 — Pressure Tap Locations for the Test Sections
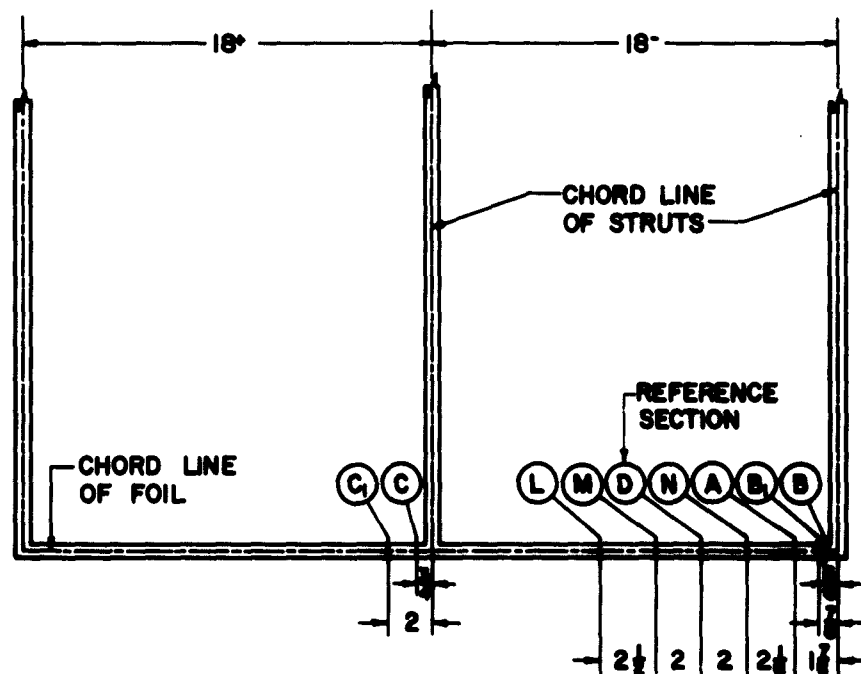
Fig. 3 — Placement of the Pressure Tap Lines in the Hydrofoil Assembly
(Assembly Viewed from Leading Edge)

Fig. 4 — Pressure Profiles at Sections Along the Foil Adjacent to an End Strut Without Fillet
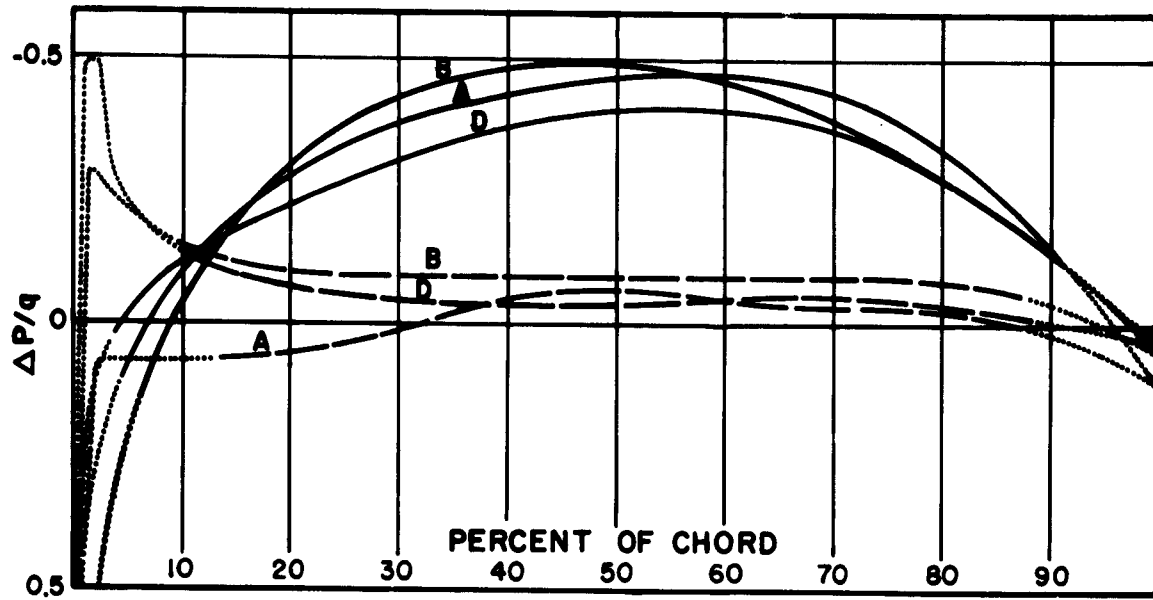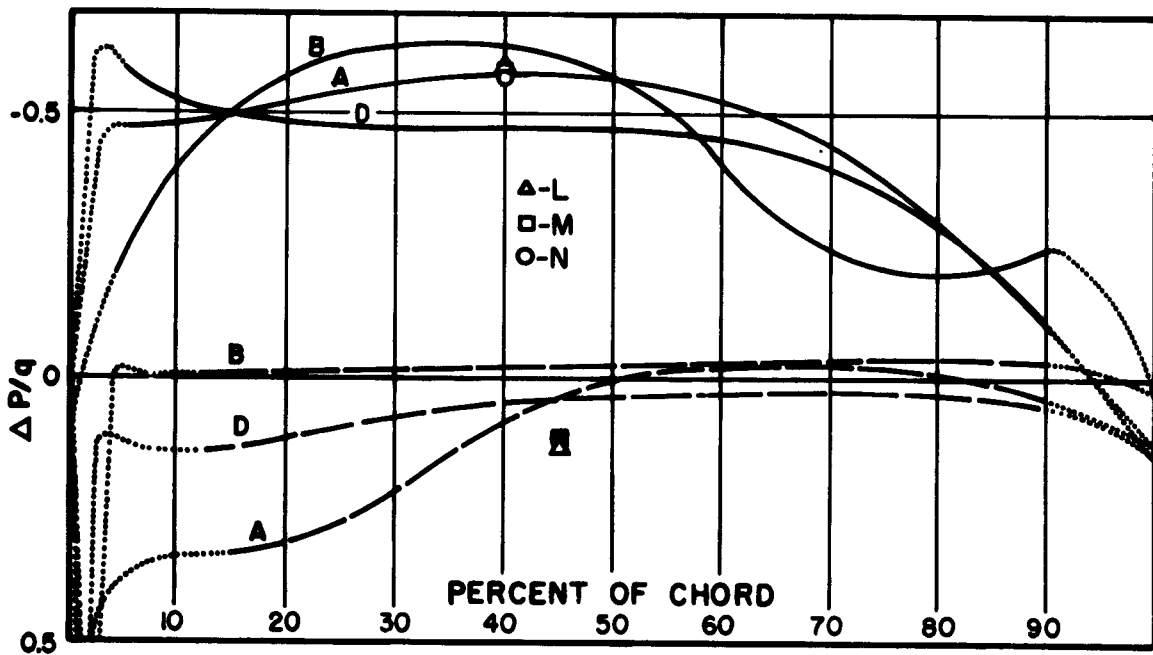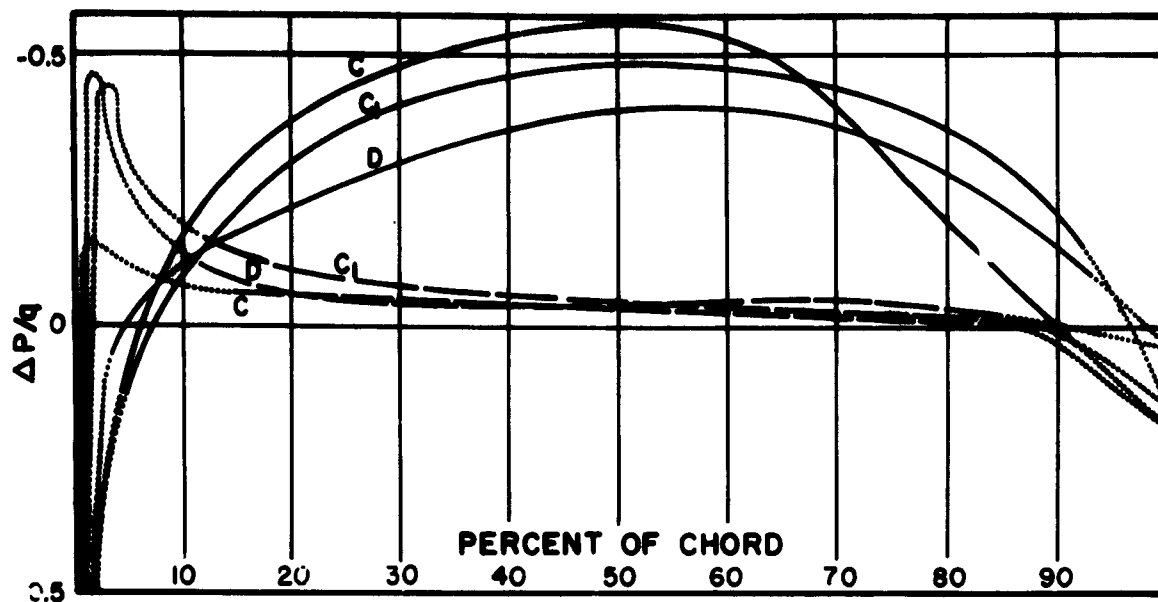
ATTACK ANGLE = 0°
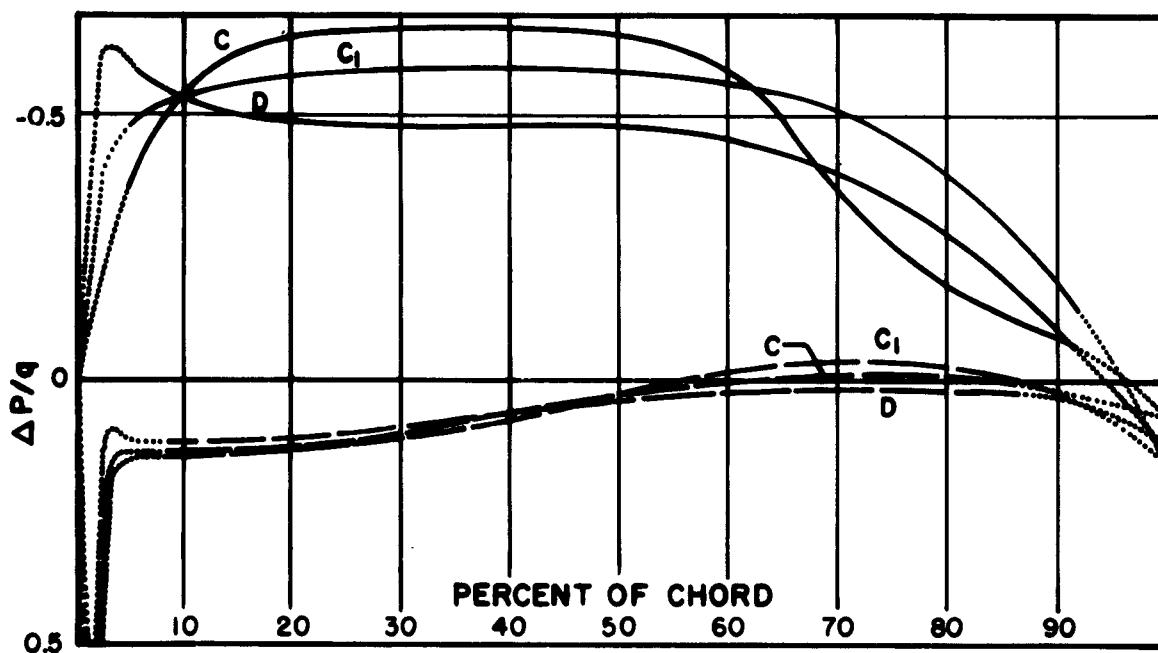
ATTACK ANGLE = 4°

R_N = 7 X 10^6
YAW ANGLE = 0°
SUBMERGENCE = 2C
LETTERS = PRESSURE LINE PER FIG.3

———————— UPPER SURFACE
— — — — LOWER SURFACE
·················· EXTRAPOLATION

Fig. 5 — Pressure Profiles at Sections Along the Foil Adjacent to a Center Strut Without Fillets

1.0

0.9

CHORD = 6 INCHES
V_0 = 14 FPS
R_N = 7 x 10^5
ψ = YAW ANGLE
H = SUBMERGENCE (%C)

0.8

0.7

MEAN LIFT COEFFICIENT, C_L

0.6

0.5

0.4

0.3

AREA MEAN VALUE WITHOUT FILLETS
—O——O— ψ =0° ; H=100
—O——O— ψ = 4° ; H=100
—△——△— ψ = 0° ; H=200
—□——□— ψ = 4° ; H=200
AREA MEAN VALUE WITH FILLETS
—◇——◇— ψ =0° ; H=100
—●——●— ψ =0° ; H=200
SECTION VALUE FROM TESTS AT LINE D
····●········●···· ψ =0° ; H=200
SECTION VALUE AT INFINITE SPAN(REF (3))
——·——·—— ψ =0° ; H=∞

0.2

0.1

0

-5° -4° -3° -2° -1° 0° 1° 2° 3° 4° 5° 6° 7° 8° 9° 10° 11°

ATTACK ANGLE

Fig. 6 - Mean Pressure Lift Coefficients of Foil 16-509 for the Area (Span = 2/3 Chord) Adjacent to an End Strut 16-012

24

MEAN DRAG COEFFICIENT, C_D

0.09
0.08
0.07
0.06
0.05
0.04
0.03
0.02
0.01
0

CHORD = 6 INCHES
V_0 = 14 FPS
R_N = 7 x 10^5
ψ = YAW ANGLE
H = SUBMERGENCE (% C)

AREA MEAN VALUE WITHOUT FILLETS
—O——O— ψ = 0° ; H = 100
—◇——◇— ψ = 4° ; H = 100
—△——△— ψ = 0° ; H = 200
—□——□— ψ = 4° ; H = 200
AREA MEAN VALUE WITH FILLETS
—◇——◇— ψ = 0° ; H = 100
—●——●— ψ = 0° ; H = 200
SECTION VALUE FROM TESTS AT LINE D
·····■····· ψ = 0° ; H = 200
SECTION VALUE AT INFINITE SPAN (REF. [3])
—·—·—· ψ = 0° ; H = ∞

ATTACK ANGLE

-5° -4° -3° -2° -1° 0° 1° 2° 3° 4° 5° 6° 7° 8° 9° 10° 11°

Fig. 7 — Mean Pressure Drag Coefficients of Foil 16–509 for the Area (Span = 2/3 Chord) Adjacent to an End Strut 16–012

Fig. 8 – Mean Pressure Lift Coefficients of Foil 16–509 for the Area (Span = 2/3 Chord) Adjacent to a Center Strut 16–012
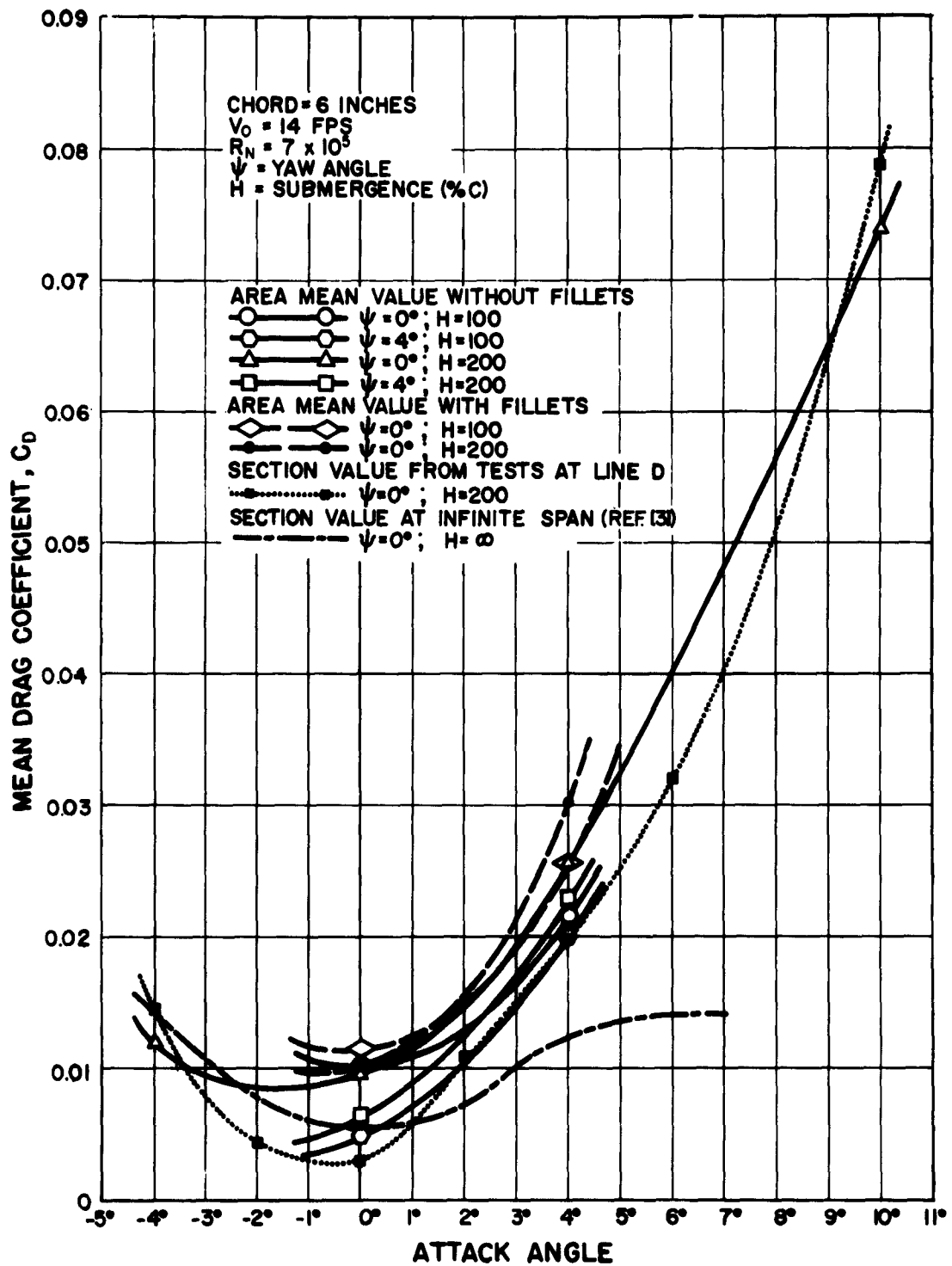
Fig. 9 — Mean Pressure Drag Coefficients of Foil 16-509 for the Area (Span = 2/3 Chord) Adjacent to a Center Strut 16-012
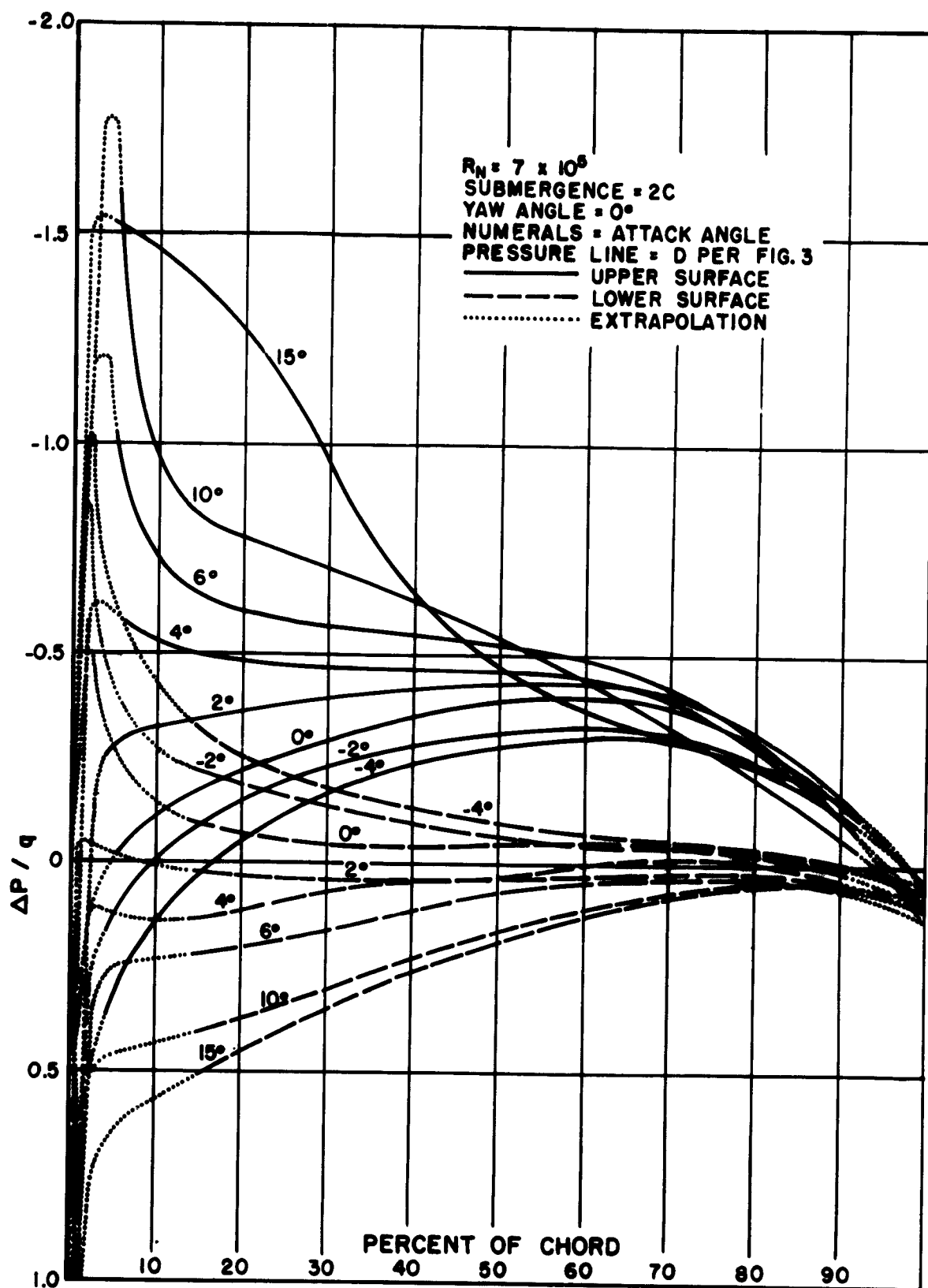
Fig. 10 — Pressure Profiles for Foil 16—509 at Tap Line D
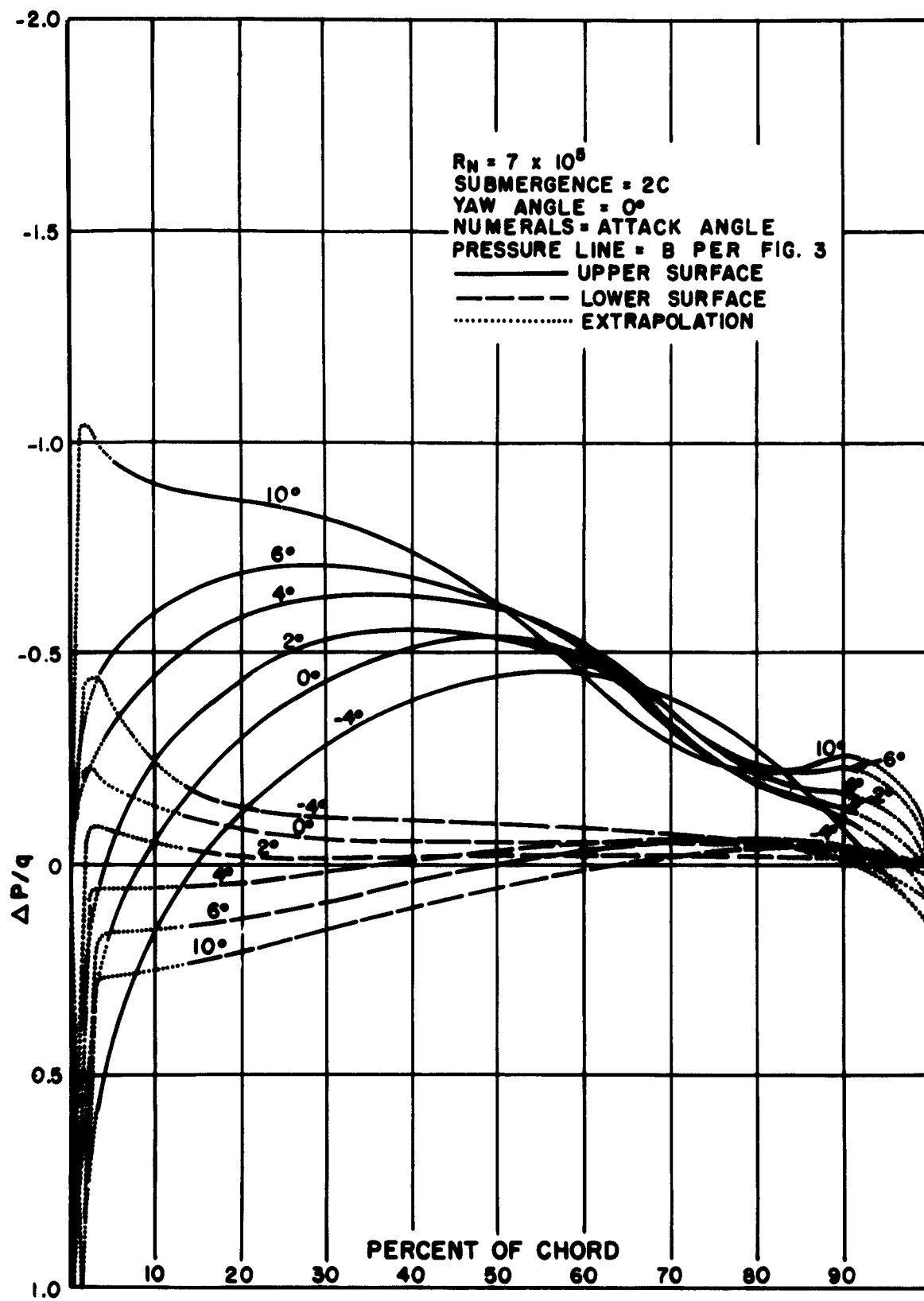
Fig. 11 - Pressure Profiles for Foil 16-509 Adjacent to an End Strut 16-012 With Fillet
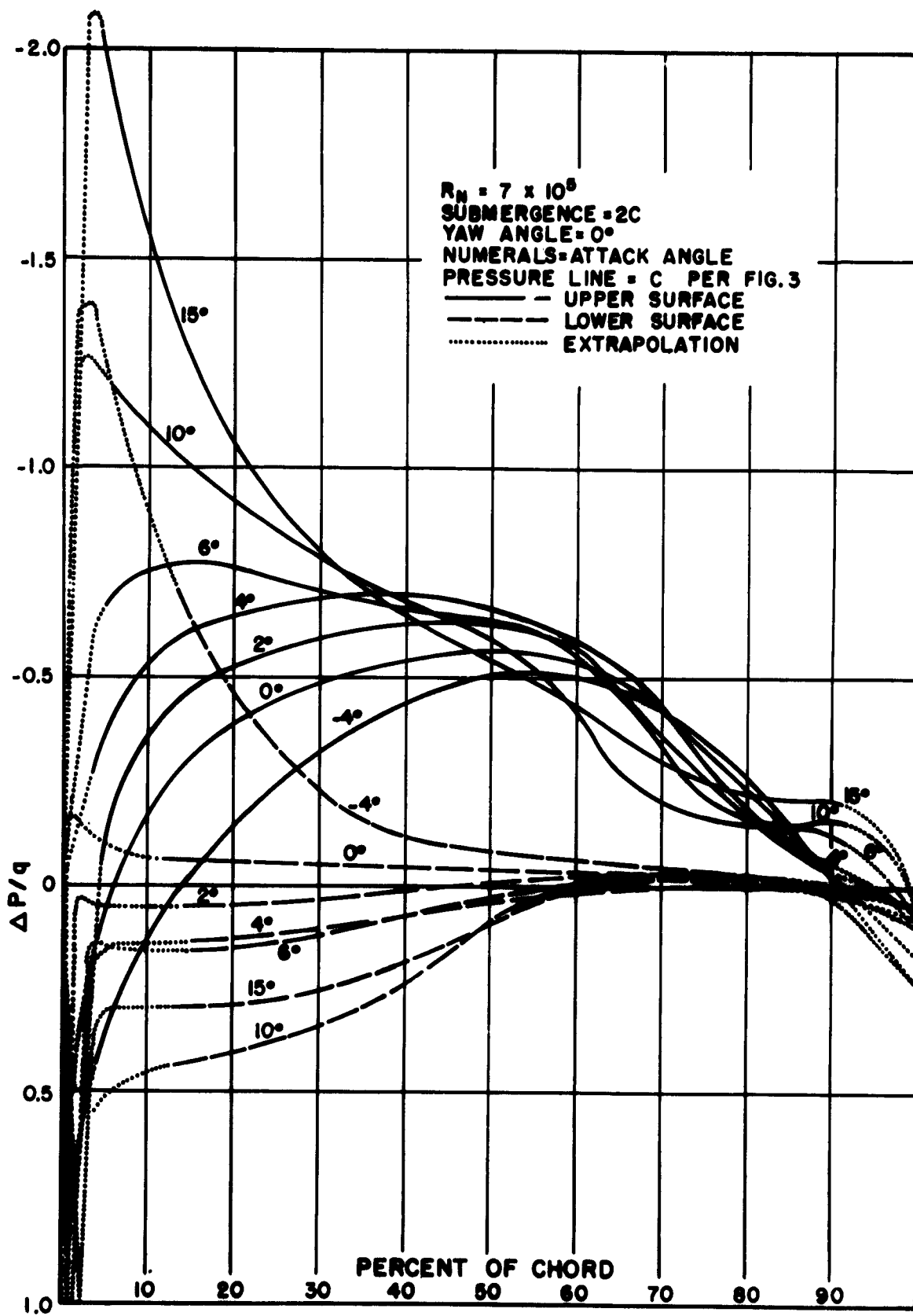
Fig. 12 — Pressure Profiles for Foil 16–509 Adjacent to a Center Strut 16–012 With Fillets
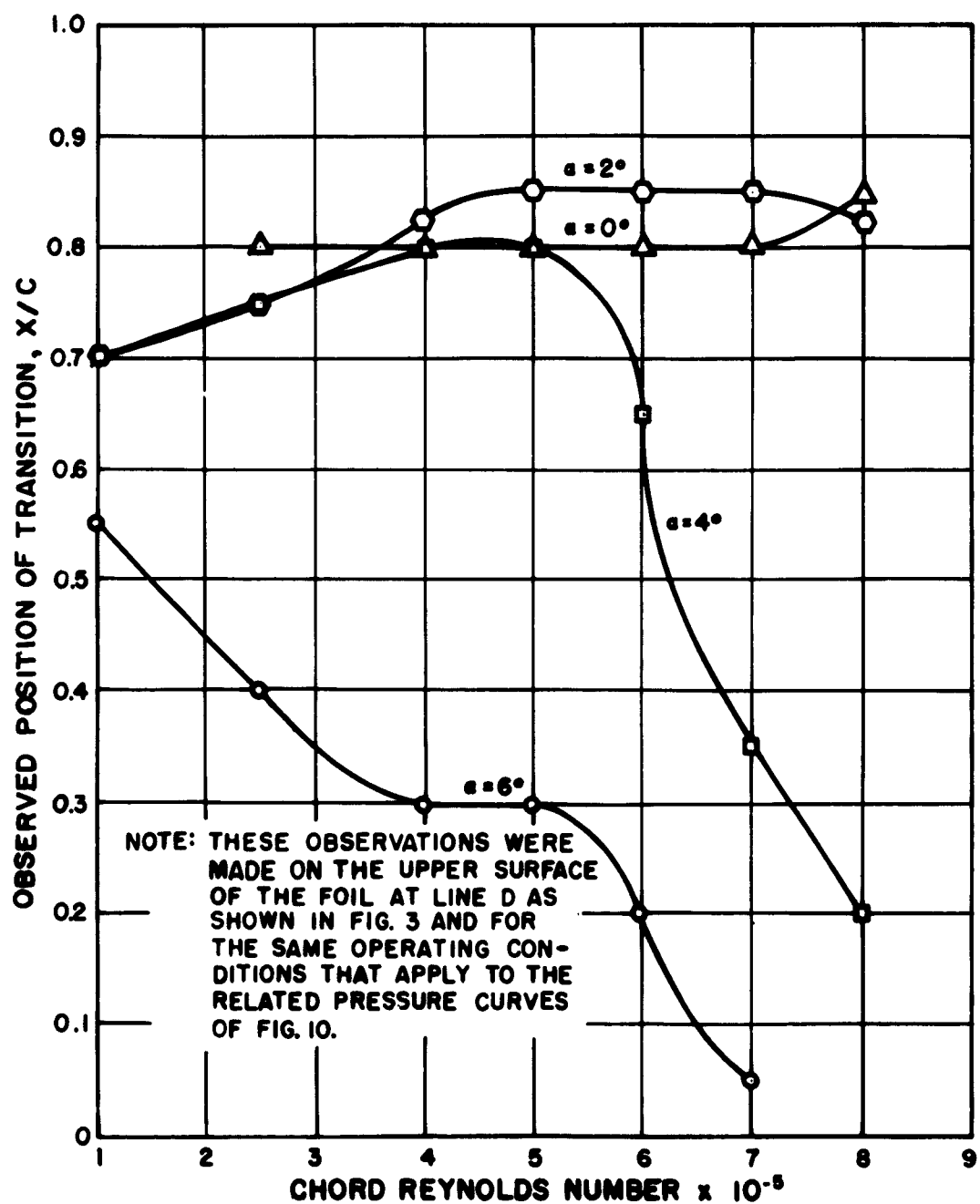
Fig. 13 - Observed Position of Boundary Layer Transition for Foil 16-509

The note within the figure reads:

NOTE: THESE OBSERVATIONS WERE MADE ON THE UPPER SURFACE OF THE FOIL AT LINE D AS SHOWN IN FIG. 3 AND FOR THE SAME OPERATING CON-DITIONS THAT APPLY TO THE RELATED PRESSURE CURVES OF FIG. 10.

LIFT PLOT

POLAR PLOT
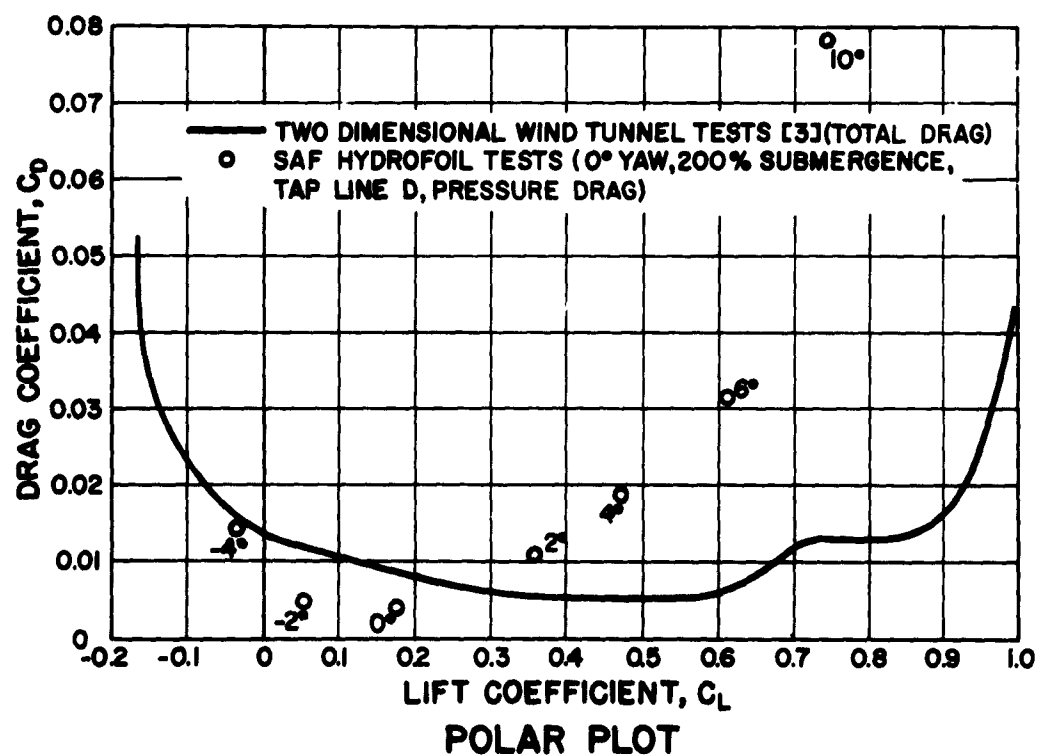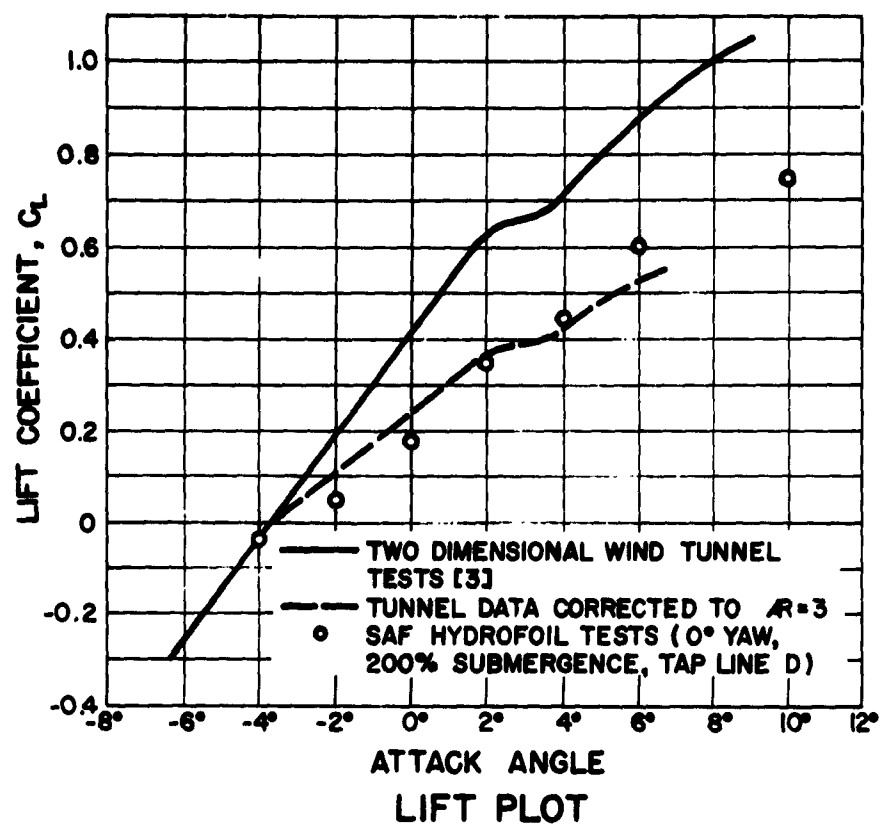
Fig. 14 – Comparative Lift and Drag Data for Foil 16–509 at Tap Line D

32
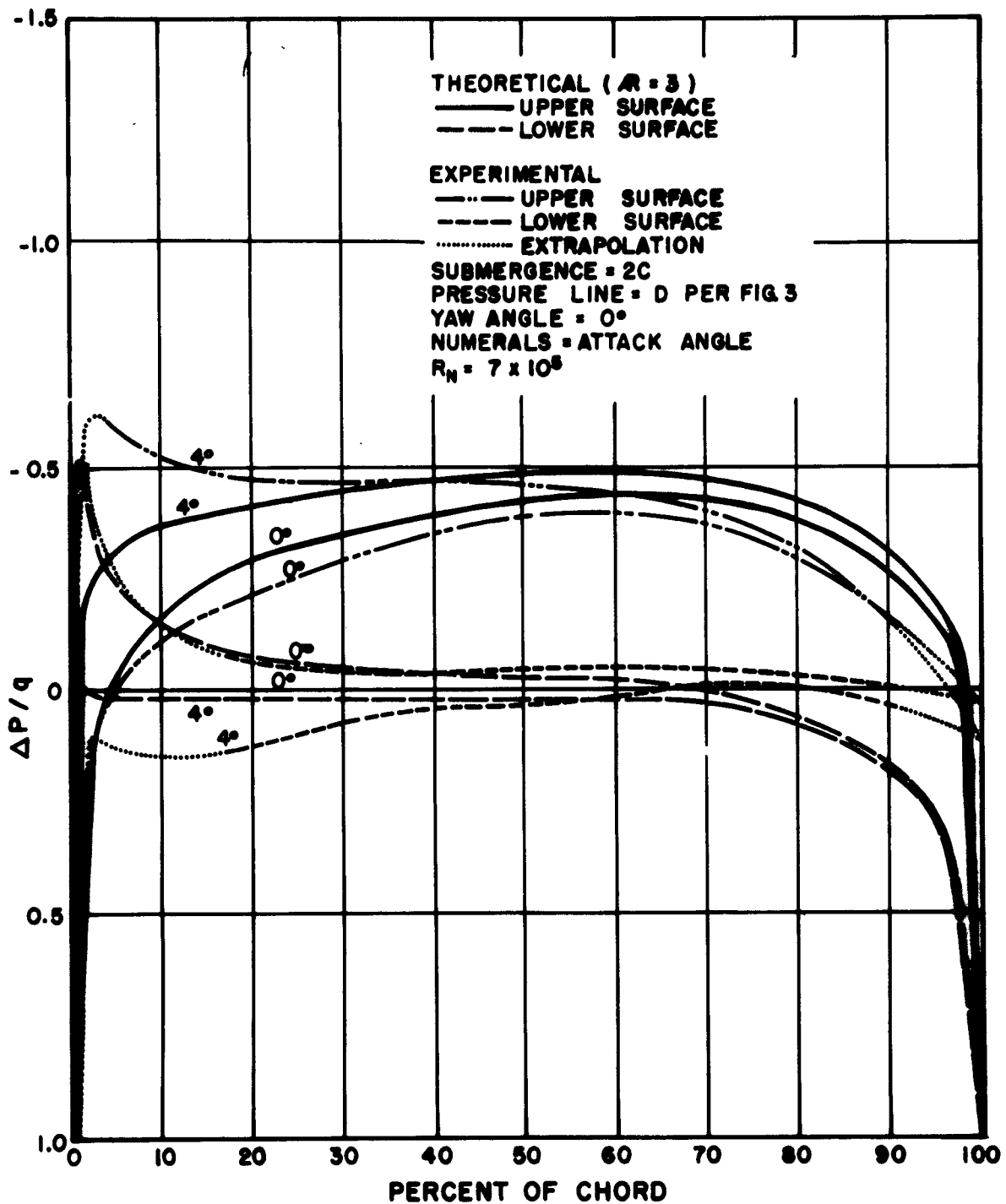
Fig. 15 — Comparative Pressure Profiles for Foil 16-509

APPENDIX

TABLE I

Coordinate Data for the Test Members

X/C per cent C	FOIL, NACA 16-509 Upper		FOIL, NACA 16-509 Lower		STRUT NACA 16-012	
	X in.	Y in.	X in.	-Y in.	X in.	Y in.
0	0	0	0	0	0	0
1.25	0.065	0.073	0.085	0.041	0.075	0.078
2.50	0.138	0.018	0.162	0.052	0.150	0.108
5.00	0.287	0.160	0.313	0.065	0.300	0.151
7.50	0.436	0.199	0.463	0.072	0.450	0.182
10	0.586	0.232	0.613	0.077	0.600	0.207
15	0.887	0.286	0.913	0.085	0.900	0.248
20	1.188	0.329	1.209	0.090	1.200	0.280
30	1.792	0.389	1.808	0.098	1.800	0.325
35			2.106	0.100	2.100	0.338
40	2.396	0.424	2.404	0.103	2.400	0.351
45			2.702	0.103	2.700	0.355
50	3.000	0.436	3.000	0.104	3.000	0.360
55	3.302	0.429			3.300	0.355
60	3.604	0.423	3.596	0.102	3.600	0.350
65	3.906	0.403			3.900	0.333
70	4.208	0.383	4.192	0.091	4.200	0.316
80	4.810	0.308	4.789	0.069	4.800	0.252
85			5.095	0.052	5.100	0.202
90	5.410	0.190	5.390	0.035	5.400	0.151
95	5.707	0.111	5.692	0.016	5.700	0.085
100	6.001	0.005	5.998	0.005	6.000	0.007

Leading Edge Radius = 0.024 in.

Leading Edge Radius = 0.042 in.

Note: The chord dimension, C, is 6 inches. The position of pressure taps in the upper and lower surfaces of the foil is underlined. A graphic treatment of this data is given in Fig. 2.

SPONSOR'S DISTRIBUTION LIST FOR PROJECT REPORT NO. 65

of the St. Anthony Falls Hydraulic Laboratory

Copies	Organisation

6   Chief of Naval Research, Department of the Navy, Washington 25, D. C., Attn:
                3 - Code 438
                1 - Code 461
                1 - Code 463
                1 - Code 466

1   Commanding Officer, Office of Naval Research, Branch Office, 495 Summer Street, Boston 10, Massachusetts.

1   Commanding Officer, Office of Naval Research, Branch Office, 346 Broadway, New York 13, New York.

1   Commanding Officer, Office of Naval Research, Branch Office, 1030 East Green Street, Pasadena, California.

1   Commanding Officer, Office of Naval Research, Branch Office, 1000 Geary Street, San Francisco 9, California.

25   Commanding Officer, Office of Naval Research, Branch Office, Navy 100, Fleet Post Office, New York, New York.

6   Director, Naval Research Laboratory, Washington 25, D. C., Attn: Code 2027.

5   Chief, Bureau of Naval Weapons, Department of the Navy, Washington 25, D. C., Attn:
                1 - Code RUAW-4
                1 - Code RRRE
                1 - Code RAAD
                1 - Code RAAD-222
                1 - Code DIS-42

9   Chief, Bureau of Ships, Department of the Navy, Washington 25, D. C., Attn:
                1 - Code 106
                1 - Code 310
                1 - Code 312
                1 - Code 335
                1 - Code 420
                1 - Code 421
                1 - Code 440
                1 - Code 442
                1 - Code 449

1   Chief, Bureau of Yards and Docks, Department of the Navy, Washington 25, D. C., Attn: Code D-400.

Copies	Organization
15	Commanding Officer and Director, David Taylor Model Basin, Washington 7, D. C., Attn:

           1 - Code 108
           1 - Code 142
           1 - Code 500
           1 - Code 513
           1 - Code 520
           1 - Code 526
           1 - Code 526A
           1 - Code 530
           1 - Code 533
           1 - Code 580
           1 - Code 585
           1 - Code 589
           1 - Code 591
           1 - Code 591A
           1 - Code 700

1	Commander, U. S. Naval Ordnance Test Station, China Lake, California, Attn: Code 753.
2	Commander, U. S. Naval Ordnance Test Station, Pasadena Annex, 3202 E. Foothill Blvd., Pasadena 8, California, Attn: Code P-508.
1	Commander, Planning Department, Portsmouth Naval Shipyard, Portsmouth, New Hampshire.
1	Commander, Planning Department, Pearl Harbor Naval Shipyard, Navy 128, Fleet Post Office, San Francisco, California.
1	Commander, Planning Department, San Francisco Naval Shipyard, San Francisco 24, California.
1	Commander, Planning Department, Mare Island Naval Shipyard, Vallejo, California.
1	Commander, Planning Department, New York Naval Shipyard, Brooklyn 1, New York.
1	Commander, Planning Department, Puget Sound Naval Shipyard, Bremerton, Washington.
1	Commander, Planning Department, Philadelphia Naval Shipyard, U. S. Naval Base, Philadelphia 12, Pennsylvania.
1	Commander, Planning Department, Norfolk Naval Shipyard, Portsmouth, Virginia.
1	Commander, Planning Department, Charleston Naval Shipyard, U. S. Naval Base, Charleston, South Carolina.

Copies	Organization
1	Commander, Planning Department, Boston Naval Shipyard, Boston 29, Massachusetts.
1	Commander, Planning Department, Long Beach Naval Shipyard, Long Beach 2, California.
1	Commander, Planning Department, U. S. Naval Weapons Laboratory, Dahlgren, Virginia.
1	Commander, U. S. Naval Ordnance Laboratory, White Oak, Maryland.
1	Dr. A. V. Hershey, Computation and Exterior Ballistics Laboratory, U. S. Naval Weapons Laboratory, Dahlgren, Virginia.
1	Superintendent, U. S. Naval Academy, Annapolis, Maryland, Attn: Library.
1	Superintendent, U. S. Naval Postgraduate School, Monterey, California.
1	Commandant, U. S. Coast Guard, 1300 E Street, N. W., Washington, D. C.
1	Secretary, Ship Structure Committee, U. S. Coast Guard Headquarters, 1300 E Street, N. W., Washington, D. C.
1	Commander, Military Sea Transportation Service, Department of the Navy, Washington 25, D. C.
3	U. S. Maritime Administration, GAO Building, 441 G Street, N. W., Washington, D. C., Attn: 1 - Division of Ship Design 1 - Division of Research 1 - Mr. R. P. Godwin
1	Superintendent, U. S. Merchant Marine Academy, Kings Point, Long Island, New York, Attn: Capt. L. S. McCready (Dept. of Engineering).
1	Commanding Officer and Director, U. S. Navy Mine Defense Laboratory, Panama City, Florida.
1	Commanding Officer, NROTC and Naval Administrative Unit, Massachusetts Institute of Technology, Cambridge 39, Massachusetts.
2	U. S. Army Transportation Research and Development Command, Fort Eustis, Virginia, Attn: Marine Transport Division.
1	Director of Research, National Aeronautics and Space Administration, 1512 H Street, N. W., Washington 25, D. C.
4	Director, Langley Research Center, Langley Field, Virginia, Attn: 2 - Mr. J. B. Parkinson 1 - Mr. I. E. Garrick 1 - Mr. D. J. Marten

Copies	Organisation

1   Director, Engineering Sciences Division, National Science Foundation, 1951 Constitution Avenue, N. W., Washington 25, D. C.

3   Director, National Bureau of Standards, Washington 25, D. C., Attn:
        1 - Fluid Mechanics Division (Dr. G. B. Schubauer)
        1 - Dr. G. H. Keulegan
        1 - Dr. J. M. Franklin

10   Armed Services Technical Information Agency, Arlington Hall Station, Arlington 12, Virginia.

1   Office of Technical Services, Department of Commerce, Washington 25, D. C.

3   California Institute of Technology, Pasadena 4, California, Attn:
        1 - Professor M. S. Plesset
        1 - Professor T. Y. Wu
        1 - Professor A. J. Acosta

1   University of California, Department of Engineering, Los Angeles 24, California, Attn: Dr. A. Powell.

1   Director, Scripps Institute of Oceanography, University of California, La Jolla, California.

1   Professor M. L. Albertson, Department of Civil Engineering, Colorado A and M College, Fort Collins, Colorado.

1   Professor J. E. Cermak, Department of Civil Engineering, Colorado State University, Fort Collins, Colorado.

1   Professor W. R. Sears, Graduate School of Aeronautical Engineering, Cornell University, Ithaca, New York.

2   State University of Iowa, Iowa Inst. of Hydraulic Research, Iowa City, Iowa, Attn:
        1 - Dr. H. Rouse
        1 - Dr. L. Landweber

2   Harvard University, Cambridge 38, Massachusetts, Attn:
        1 - Professor G. Birkhoff (Dept. of Mathematics)
        1 - Professor G. F. Carrier (Dept. of Mathematics)

2   Massachusetts Institute of Technology, Cambridge 39, Massachusetts, Attn:
        1 - Department of Naval Architecture and Marine Engineering
        1 - Professor A. T. Ippen

3   University of Michigan, Ann Arbor, Michigan, Attn:
        1 - Professor R. B. Couch (Dept. of Naval Architecture)
        1 - Professor W. W. Willmarth (Aero. Engrg. Department)
        1 - Professor M. S. Uberoi (Aero. Engrg. Department)

Copies	Organisation

3   Dr. L. G. Straub, Director, St. Anthony Falls Hydraulic Lab, University of Minnesota, Minneapolis 14, Minnesota, Attn:
      1 - Dr. Straub
      1 - Mr. J. M. Wetzel
      1 - Professor E. Silberman

1   Professor J. J. Foody, Engineering Department, New York State University Maritime College, Fort Schulyer, New York.

3   New York University, Institute of Mathematical Sciences, 25 Waverly Place, New York 3, New York, Attn:
      1 - Professor J. Keller
      1 - Professor J. J. Stoker
      1 - Professor R. Kraichnan

3   The Johns Hopkins University, Department of Mechanical Engineering, Baltimore 18, Maryland, Attn:
      1 - Professor S. Corrsin
      2 - Professor O. M. Phillips

1   Massachusetts Institute of Technology, Department of Naval Architecture and Marine Engineering, Cambridge 39, Massachusetts, Attn: Prof. M. A. Abkowitz, Head.

2   Dr. G. F. Wislicenus, Ordnance Research Laboratory, Pennsylvania State University, University Park, Pennsylvania, Attn:
      1 - Dr. Wislicenus
      1 - Dr. M. Sevik

1   Professor R. C. DiPrima, Department of Mathematics, Rensselaer Polytechnic Institute, Troy, New York.

5   Stevens Institute of Technology, Davidson Laboratory, Castle Point Station, Hoboken, New Jersey, Attn:
      1 - Professor E. V. Lewis
      1 - Mr. D. Savitsky
      1 - Mr. J. P. Breslin
      1 - Mr. C. J. Henry
      1 - Mr. S. Tsakonas

1   Webb Institute of Naval Architecture, Crescent Beach Road, Glen Cove, New York, Attn: Technical Library.

1   Director, Woods Hole Oceanographic Institute, Woods Hole, Massachusetts.

1   Executive Officer, Air Research and Development Command, Air Force Office of Scientific Research, Washington 25, D. C., Attn: Mechanics Branch.

1   Commander, Wright Air Development Division, Aircraft Laboratory, Wright-Patterson Air Force Base, Ohio, Attn: Mr. W. Mykytow, Dynamics Branch.

Copies	Organisation

2   Cornell Aeronautical Laboratory, 4455 Genesee Street, Buffalo, New York, Attn:
        1 - Mr. W. Targoff
        1 - Mr. R. White

3   Massachusetts Institute of Technology, Fluid Dynamics Research Laboratory, Cambridge 39, Massachusetts, Attn:
        1 - Professor H. Ashley
        1 - Professor M. Landahl
        1 - Professor J. Dugundji

2   Hamburgische Schiffbau-Versuchsanstalt, Bramfelder Strasse 164, Hamburg 33, Germany, Attn:
        1 - Dr. O. Grim
        1 - Dr. H. W. Lerbs

1   Institut fur Schiffbau der Universitat Hamberg, Berliner Tor 21, Hamburg 1, Germany, Attn: Professor G. P. Weinblum, Director.

1   Max-Planck Institut fur Stromungsforschung, Bottingerstrasse 6/8, Gottingen, Germany, Attn: Dr. H. Reichardt.

1   Hydro-og Aerodynamisk Laboratorium, Lyngby, Denmark, Attn: Professor Carl Prohaska.

1   Skipsmodelltanken, Trondheim, Norway, Attn: Professor J. K. Lunde.

1   Versuchsanstalt fur Wasserbau und Schiffbau, Schleuseninsel im Tiergarten, Berlin, Germany, Attn: Dr. S. Schuster, Director.

1   Technische Hogeschool, Institut voor Toegepaste Wiskunde, Julianalaan 132, Delft, Netherlands, Attn: Professor R. Timman.

1   Netherlands Ship Model Basin, Wageningen, Netherlands, Attn: Dr. Ir. J. D. van Manen.

1   Allied Research Associates, Inc., 43 Leon Street, Boston 15, Massachusetts, Attn: Dr. T. R. Goodman.

3   National Physical Laboratory, Teddington, Middlesex, England, Attn:
        1 - Dr. F. H. Todd, Superintendent Ship Division
        1 - Head Aerodynamics Division
        1 - Mr. A. Silverleaf

2   Head, Aerodynamics Department, Royal Aircraft Establishment, Farnborough, Hants, England, Attn: Mr. M. O. W. Wolfe.

1   Boeing Airplane Co., Seattle Division, Seattle, Washington, Attn: Mr. M. J. Turner.

1   Electric Boat Division, General Dynamics Corporation, Groton, Connecticut, Attn: Mr. Robert McCandliss.

Copies	Organization
1	General Applied Sciences Labs, Inc., Merrick and Stewart Avenues, Westbury, Long Island, New York.
1	Gibbs and Cox, Inc., 21 West Street, New York, New York.
2	Grumman Aircraft Engineering Corp., Bethpage, Long Island, New York, Attn: 1 - Mr. E. Baird 1 - Mr. E. Bower
1	Grumman Aircraft Engineering Corp., Dynamic Developments Division, Babylon, New York.
1	Lockheed Aircraft Corporation, Missiles and Space Division, Palo Alto, California, Attn: R. W. Kermeen.
1	Midwest Research Institute, 425 Volker Blvd., Kansas City 10, Missouri, Attn: Mr. Zeydel.
3	Director, Department of Mechanical Sciences, Southwest Research Institute, 8500 Culebra Road, San Antonio 6, Texas, Attn: 1 - Dr. H. N. Abramson 1 - Mr. G. Ransleben 1 - Editor, Applied Mechanics Review
3	Convair, A Division of General Dynamics, San Diego, California, Attn: 1 - Mr. R. H. Oversmith 1 - Mr. A. D. MacLellan 1 - Mr. H. E. Brooke
1	Dynamic Developments, Inc., 15 Berry Hill Road, Oyster Bay, Long Island, New York.
1	Dr. S. F. Hoerner, 148 Busteed Drive, Midland Park, New Jersey.
1	Hydronautics, Incorporated, 200 Monroe Street, Rockville, Maryland, Attn: Mr. Phillip Eisenberg.
1	Rand Development Corporation, 13600 Deise Avenue, Cleveland 10, Ohio, Attn: Dr. A. S. Iberall.
1	U. S. Rubber Company, Research and Development Department, Wayne, New Jersey, Attn: Mr. L. M. White.
1	Technical Research Group, Inc., 2 Aerial Way, Syosset, Long Island, New York, Attn: Mr. Jack Kotik.
1	Mr. C. Wigley, Flat 102, 6-9 Charterhouse Square, London, E. C. 1, England.
1	AVCO Corporation, Lycoming Division, 1701 K Street, N. W., Apt. 904, Washington, D. C., Attn: Mr. T. A. Duncan.

Copies	Organization
1	Mr. J. G. Baker, Baker Manufacturing Company, Evansville, Wisconsin.
1	Curtiss-Wright Corporation Research Division, Turbomachinery Division, Quehanna, Pennsylvania, Attn: Mr. George H. Pedersen.
1	Hughes Tool Company, Aircraft Division, Culver City, California, Attn: Mr. M. S. Harned.
1	Lockheed Aircraft Corporation, California Division, Hydrodynamics Research, Burbank, California, Attn: Mr. Bill East.
1	National Research Council, Montreal Road, Ottawa 2, Canada, Attn: Mr. E. S. Turner.
1	The Rand Corporation, 1700 Main Street, Santa Monica, California, Attn: Dr. Blaine Parkin.
2	Stanford University, Department of Civil Engineering, Stanford, California, Attn: 1 - Dr. Byrne Perry 1 - Dr. E. Y. Hsu
1	Waste King Corporation, 5550 Harbor Street, Los Angeles 22, California, Attn: Dr. A. Schneider.
1	Commanding Officer, Office of Naval Research Branch Office, The John Crerar Library Bldg., 86 E. Randolph Street, Chicago 1, Illinois.
1	Commanding Officer and Director, U. S. Naval Engineering Experiment Station, Annapolis, Maryland.
1	Commanding Officer, U. S. Naval Underwater Ordnance Station, Newport, Rhode Island, Attn: Research Division.
1	National Academy of Sciences, National Research Council, 2101 Constitution Avenue, N. W., Washington 25, D. C.
1	Commanding Officer, U. S. Army Research Office, Box CM, Duke Station, Durham, North Carolina.
2	University of California, Berkeley 4, California, Attn: 1 - Department of Engineering 1 - Prof. H. A. Schade
1	Society of Naval Architects and Marine Engineers, 74 Trinity Place, New York 6, New York.
1	Engineering Societies Library, 29 W. 39th Street, New York 18, New York.
1	EDO Corporation, College Point, L. I., New York.

Copies	Organization
1	Director of Research, National Aeronautics and Space Administration, Lewis Research Center, 21000 Brookpark Road, Cleveland 35, Ohio.
1	Commanding Officer and Director, U. S. Naval Civil Engineering Laboratory, Port Hueneme, California, Attn: Code L54.
1	Dr. Hirsh Cohen, IBM Research Center, PO Box 218, Yorktown Heights, New York.
1	Mr. David Wellinger, Hydrofoil Projects, Radio Corporation of America, Burlington, Massachusetts.
1	Prof. Ir. J. Gerritsma, Technische Hogeschool, Onderafdeling der Scheepsbouwkunde, Prof. Mekelweg 2, Delft, The Netherlands.
1	Dr. H. Schwanecke, Versuchsanstalt fur Wasserbau und Schiffbau, Schleuseninsel in Tiergarten, Berlin, Germany.
1	Bureau D'Analyse et de Recherche Appliquees, 47 avenue Victor Cresson - Issy des Moulineaux (Seine), Paris, France, Attn: Prof. L. Malavard.